limitation for the oligomers described here is that library members assembled from fewer building blocks have an entropic advantage over species assembled from a larger number of building blocks. Although template binding energy can overcome this disadvantage, such a handicap could make the assembly of long oligomers challenging. It remains to be seen whether the sequence integrity of the tPNA oligomers will be sufficient to propagate genetic information through multiple rounds of replication or templated synthesis.

References and Notes

1. G. K. Mittapalli *et al.*, *Angew. Chem. Int. Ed.* **46**, 2478 (2007).
2. S. Karkare, D. Bhatnagar, *Appl. Microbiol. Biotechnol.* **71**, 575 (2006).
3. A. Eschenmoser, *Chimia (Aarau)* **59**, 836 (2005).
4. L. Zhang, A. Peritz, E. Meggers, *J. Am. Chem. Soc.* **127**, 4174 (2005).
5. F. Beck, P. E. Nielsen, in *Artificial DNA*, Y. E. Khudyakov, H. A. Fields, Eds. (CRC Press, Boca Raton, FL, 2003), pp. 91–114.
6. U. Diederichsen, *Angew. Chem. Int. Ed. Engl.* **35**, 445 (1996).
7. R. E. Kleiner, Y. Brudno, M. E. Birnbaum, D. R. Liu, *J. Am. Chem. Soc.* **130**, 4646 (2008).
8. D. A. Fulton, *Org. Lett.* **10**, 3291 (2008).
9. D. T. Hickman, N. Sreenivasachary, J.-M. Lehn, *Helv. Chim. Acta* **91**, 1 (2008).
10. S. Ladame, *Org. Biomol. Chem.* **6**, 219 (2008).
11. P. T. Corbett *et al.*, *Chem. Rev.* **106**, 3652 (2006).
12. N. Sreenivasachary, D. T. Hickman, D. Sarazin, J.-M. Lehn, *Chem. Eur. J.* **12**, 8581 (2006).
13. W. G. Skene, J.-M. P. Lehn, *Proc. Natl. Acad. Sci. U.S.A.* **101**, 8270 (2004).
14. Y. Higaki, H. Otsuka, A. Takahara, *Macromolecules* **37**, 1696 (2004).
15. S. J. Rowan, S. J. Cantrill, G. R. L. Cousins, J. K. M. Sanders, J. F. Stoddart, *Angew. Chem. Int. Ed.* **41**, 899 (2002).
16. X. Li, D. G. Lynn, *Angew. Chem. Int. Ed.* **41**, 4567 (2002).
17. K. Oh, K.-S. Jeong, J. S. Moore, *Nature* **414**, 889 (2001).
18. Z.-Y. J. Zhan, D. G. Lynn, *J. Am. Chem. Soc.* **119**, 12420 (1997).
19. J. T. Goodwin, D. G. Lynn, *J. Am. Chem. Soc.* **114**, 9197 (1992).
20. N. V. Hud, S. S. Jain, X. Li, D. G. Lynn, *Chem. Biodivers.* **4**, 768 (2007).
21. R. Pascal, L. Boiteau, A. Commeyras, *Top. Curr. Chem.* **259**, 69 (2005).
22. J.-P. Biron, A. L. Parkes, R. Pascal, J. D. Sutherland, *Angew. Chem. Int. Ed.* **44**, 6731 (2005).
23. L. E. Orgel, *Crit. Rev. Biochem. Mol. Biol.* **39**, 99 (2004).
24. C. De Duve, in *Molecular Origins of Life*, A. Brack, Ed. (Cambridge Univ. Press, Cambridge, 1998), pp. 219–236.
25. Materials and methods are available as supporting online material on *Science* Online.
26. J. Leclaire, L. Vial, S. Otto, J. K. M. Sanders, *Chem. Commun. (Camb.)* **15**, 1959 (2005).
27. M. G. Woll, S. H. Gellman, *J. Am. Chem. Soc.* **126**, 11172 (2004).
28. R. Larsson, Z. Pei, O. Ramström, *Angew. Chem. Int. Ed.* **43**, 3716 (2004).
29. H. D. Bean, F. A. L. Anet, I. R. Gould, N. V. Hud, *Orig. Life Evol. Biosph.* **36**, 39 (2006).
30. P. T. Corbett, J. K. M. Sanders, S. Otto, *Chem. Eur. J.* **14**, 2153 (2008).
31. P. T. Corbett, S. Otto, J. K. M. Sanders, *Chem. Eur. J.* **10**, 3139 (2004).
32. K. Severin, *Chem. Eur. J.* **10**, 2565 (2004).
33. A. Grote, R. Scopelliti, K. Severin, *Angew. Chem. Int. Ed.* **42**, 3821 (2003).
34. This work is dedicated in memory of our friend and colleague Professor Leslie E. Orgel (1927–2007). We thank R. Krishnamurthy and A. Eschenmoser for helpful discussions. Support was provided in part by the Skaggs Institute for Chemical Biology, the NASA Earth and Space Science Fellowship Program (grant NNX07AR35H to J.M.B.), and the NASA Science Mission Directorate's Planetary Science Division (NRA NNH07ZDA001N).

Impact of Shifting Patterns of Pacific Ocean Warming on North Atlantic Tropical Cyclones

Hye-Mi Kim, Peter J. Webster,* Judith A. Curry

Two distinctly different forms of tropical Pacific Ocean warming are shown to have substantially different impacts on the frequency and tracks of North Atlantic tropical cyclones. The eastern Pacific warming (EPW) is identical to that of the conventional El Niño, whereas the central Pacific warming (CPW) has maximum temperature anomalies located near the dateline. In contrast to EPW events, CPW episodes are associated with a greater-than-average frequency and increasing landfall potential along the Gulf of Mexico coast and Central America. Differences are shown to be associated with the modulation of vertical wind shear in the main development region forced by differential teleconnection patterns emanating from the Pacific. The CPW is more predictable than the EPW, potentially increasing the predictability of cyclones on seasonal time scales.

North Atlantic tropical cyclones (hereafter "cyclones") have a substantial societal impact in the United States, Mesoamerica, and the Caribbean, and much effort has been expended in predicting their number and frequency (*1–4*). Over the past 150 years, U.S. landfall frequencies and damages have been smaller during El Niño ($800 million/year) than during La Niña ($1600 million/year) (*5*). The phase of the El Niño Southern Oscillation (ENSO) is a critical predictor used in empirical forecasting of the number of cyclones (*1, 6, 7*). Correlations between the phase of ENSO and cyclone activity have been well documented: Activity is reduced in the El Niño phase whereas it is increased in the La Niña phase, which is attributed to alterations in vertical wind shear (*1*) or atmospheric stability (*8*) associated with the different phases of ENSO.

Several recent studies (*9–13*) have identified episodes of warming in the central Pacific Ocean (central Pacific warming, CPW), in contrast to the conventional El Niño warming that occurs generally in the cold tongue region of the East Pacific Ocean (eastern Pacific warming, EPW). Warming and cooling events are defined based on the detrended sea-surface temperature (SST) (*14*) anomaly index for August to October, as discussed in the Supporting Online Material (SOM). EPW, CPW, and Eastern Pacific cooling (EPC) events are defined as follows: Niño 3 (fig. S1) warming greater than 1 standard deviation (SD),

for EPW; Niño 3 or Niño 3.4 cooler than 1 SD, for EPC; and for CPW, Niño 4 warming exceeding 1 SD, while Niño 3 stays below this range. The results are shown in fig. S2.

With these definitions, a total of 9 EPW years, 5 CPW years, and 12 EPC years were identified. SST anomalies for all warming events since 1950 are shown in fig. S3. Although the frequency of the total number of warm events (i.e., CPW + EPW) has stayed approximately the same, the occurrence of CPW events has been increasing at the expense of EPW events, especially since the early 1990s (fig. S2). The frequency of cold-phase events (EPC) has remained approximately the same.

Figure 1, A to C, displays the composite of SST anomalies during the period August to October for EPW, CPW, and EPC events, respectively. The CPW (Fig. 1B) is confined to the central Pacific with a maximum SST anomaly near the dateline, whereas EPW events (Fig. 1A) are located 60° to 80° to the east, in a location similar to that of the EPC maximum negative anomaly (Fig. 1C). The magnitude of the CPW anomaly is smaller than that associated with EPW but is set against a higher background SST, making it possibly more conducive to the formation of deep convection. Remote climate associations during CPW and EPW have been found to be different (*11*). For example, a CPW event appears to be associated with reduced rainfall in the western United States and increased rainfall in the eastern United States, opposite to that expected during an EPW (*15*).

The monthly variation in the frequency of tropical cyclone formation from June to November is shown in Fig. 1D for EPW, CPW, and EPC, in addition to the climatological average, using the National Hurricane Center Best Track tropical

School of Earth and Atmospheric Science, Georgia Institute of Technology, 311 Ferst Drive, Atlanta, GA 30332, USA.

*To whom correspondence should be addressed. E-mail: pjw@eas.gatech.edu
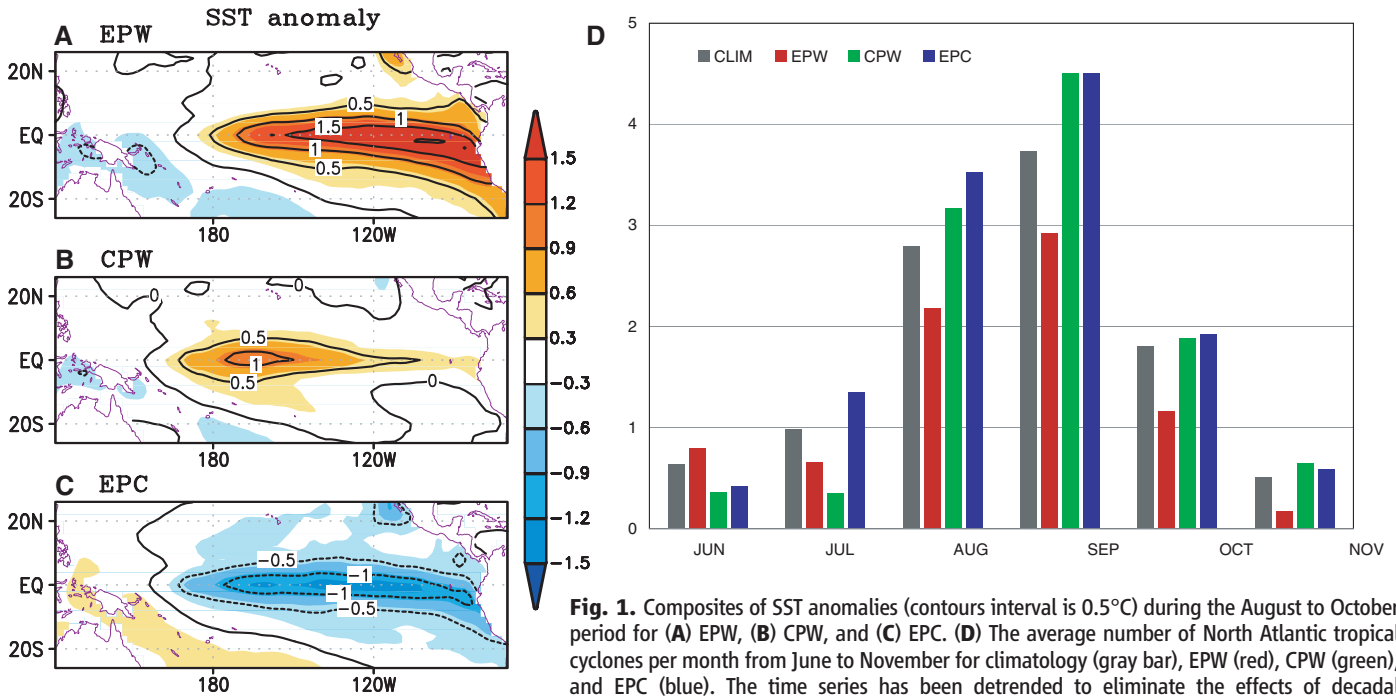
Fig. 1. Composites of SST anomalies (contours interval is 0.5°C) during the August to October period for (**A**) EPW, (**B**) CPW, and (**C**) EPC. (**D**) The average number of North Atlantic tropical cyclones per month from June to November for climatology (gray bar), EPW (red), CPW (green), and EPC (blue). The time series has been detrended to eliminate the effects of decadal variability or climate trends.

cyclone database (*16*) from 1950 to 2006. The database was detrended to avoid the possible statistical influence of a climate trend (*17–19*) or decadal variability (*20, 21*). Climatologically, the greatest number of cyclones occurs during August to October. There is a clear difference between the number of cyclones forming during EPW and EPC events, as noted earlier (*1*), but there is almost as large a difference between the EPW and CPW events. The accumulated cyclone energy (ACE) also shows that the overall cyclone activity is larger in CPW events than in EPW events (table S1).

The location of the Pacific warming also affects the location of cyclogenesis and the tracks of tropical cyclones. Figure 2 shows the composite of mean track density anomalies relative to the 57-year climatology. To calculate the track density, "best track" locations are binned into 5° × 5° grid boxes. Track density for a specific type of Pacific warming or cooling event is defined as the number of cyclones passing through each grid box during the ASO period divided by the total number of years for that type of event. Track density is smoothed by averaging the eight-grid points surrounding the main grid point with 1:8 weighting and the total divided by 2. This technique provides anomaly patterns of the locus of tropical storms (*22*). A bootstrap technique (*23*) is applied to determine statistical significance of the track density. For the EPW events, a composite anomaly is constructed with 9 years chosen at random from among the 57 years of data. The process is repeated 10,000 times to obtain a probability distribution at 90 and 95% levels. The same process is applied for CPW but by choosing 5 years and, for EPC, 12 years. Confidence limits

are shown as contours on Fig. 2. During an EPW (Fig. 2A), track density is reduced over most of the North Atlantic, with a concentration in the western and Caribbean regions. The tracks during a CPW event (Fig. 2B) differ markedly from those occurring during an EPW event: Compared to climatology, track density for CPW increases across the Caribbean, the Gulf of Mexico, and the U.S. east coast, but it decreases in the central and western North Atlantic. During an EPC event (Fig. 2C), large increases in track density occur across the entire North Atlantic.

The year 2004 was a CPW year. Seasonal cyclone forecasts predicted lower-than-average activity based on predictions of El Niño by the National Oceanic and Atmospheric Administration Climate Prediction Center (*24*) using the Niño 3.4 index. However, the cyclone activity was unusually high, contrary to normal expectations for an El Niño year. A total of 15 tropical cyclones developed in the North Atlantic, of which 12 were named storms. In 2004, tropical cyclones caused a total of $40 billion in damage and led to the loss of 3000 lives. There was a concentration of cyclones in the Caribbean and the Gulf of Mexico. Also, 2002 was a CPW year. The number of landfalling cyclones was again higher than expected in an El Niño year. ACE was below average, but the track density anomaly was close to that shown in Fig. 2B.

The differences in cyclone tracks for EPW, CPW, and EPC are consistent with changes in atmospheric circulation caused by differential heating in the Pacific that forces changes in vertical shear in the main development region of the North Atlantic (5°N to 20°N, 85°W to 15°W). Figure S4 shows that the wind shear (the difference in

zonal wind speed between 200 and 850 hPa) is stronger during EPW periods and weaker during EPC periods, whereas during CPW periods the wind shear anomaly is almost neutral. Strengthening or weakening of the vertical wind shear occurs largely through changes in the upper-level westerly flow (fig. S5) and is thought to be a major factor inhibiting or enhancing the formation and intensification of cyclones (*1*).
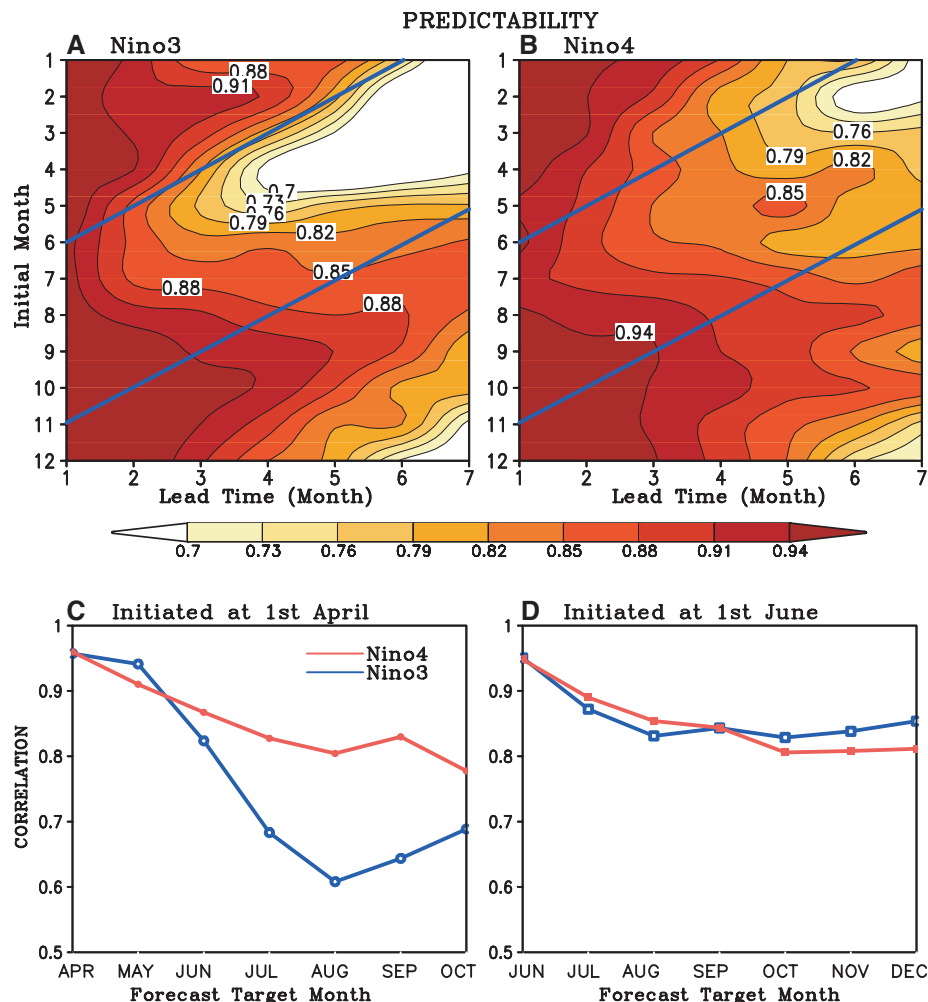
We have shown that there are statistically significant differences between the frequency and tracks of cyclones during EPW compared to CPW events. For these associations to be useful in seasonal prediction, the location of the anomalous Pacific warming needs to be forecast well in advance of the hurricane season. Prediction of the Niño 3.4 and Niño 3 (e.g., EPW) is hampered by the existence of a "predictability barrier" (*25–27*) that limits the prediction of Niño 3.4 or 3 before April or May. To perform an initial assessment of the relative predictability of EPW and CPW, we compare the predictability of Niño 3 (indicative of an EPW event) and Niño 4 index (indicative of a CPW event) using the ECMWF Seasonal Forecasting System (see SOM) (*28*). On the first day of each calendar month in the period 1981 to 2007, 11 7-month ensembles were generated, giving a total of 3564 7-month integrations. The results of this "serial integration" are shown in Fig. 3 as anomaly correlations in ensemble mean as a function of lead time (1 to 7 months) for the entire year. The two bold diagonal lines indicate target months June and November, framing the North Atlantic hurricane season. We define useful predictability occurring when correlations are greater than 0.7. The Niño 3 (or EPW) predictability (Fig. 3A)

Track density anomaly
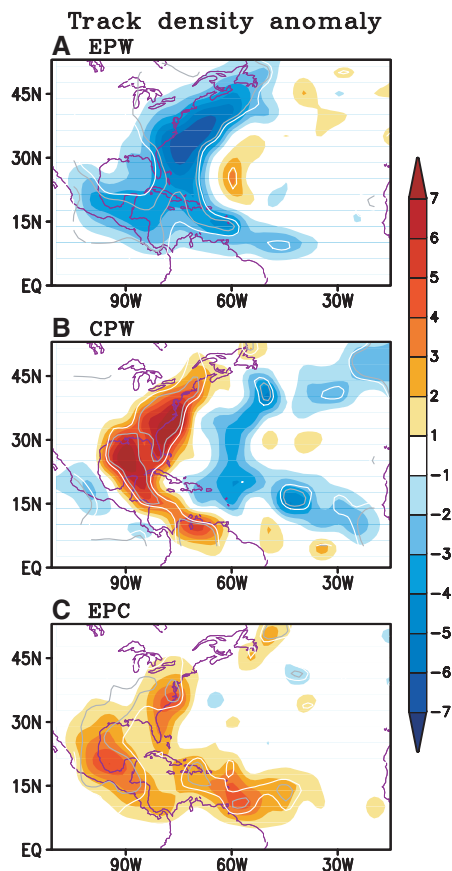
A EPW

B CPW

C EPC

Fig. 2. Composites of track density anomaly (multiplied by 10) during the August to October period for (**A**) EPW, (**B**) CPW, and (**C**) EPC. Light (dark) contours show statistical significance at the 90% (95%) level.

PREDICTABILITY

A Nino3

B Nino4

C Initiated at 1st April

D Initiated at 1st June

Fig. 3. Estimates of the predictability of EPW and CPW events. Correlations between predicted and observed values of SST anomalies for the (**A**) Niño 3 and (**B**) Niño 4 regions (fig. S1) as a function of initial month and lead-time. The predictability target zone for the period June through November (the North Atlantic tropical cyclone season) lies between the two blue diagonal lines. (**C** and **D**) Correlation of hindcasts initiated on 1 April and 1 June. Niño 4 (or CPW) possesses useful predictability for the target zone 2 to 3 months in advance of Niño 3 (or EPW).

shows clear seasonality, with the spring predictability diminishing rapidly into the hurricane season target months. Hindcasts made earlier than May provide little information about the ensuing hurricane season. By contrast, the Niño 4 (or CPW) predictability (Fig. 3B) has no obvious spring barrier. Figure 3, C and D, showing hindcasts initialized on 1 April and 1 June, indicate extended predictability earlier in the season for CPW than for EPW.

At present, it is difficult to assess why there has been an increased frequency of CPW events during the past few decades while EPW events have declined. Determining whether the CPW is a new mode associated with a general warming of the tropical oceans, or is connected to decadal modes of Pacific variability that have strong SST expressions in the central tropical Pacific such as the North Pacific Gyre Oscillation (29), is hampered by both data and model inadequacies. Many of the models used in the Intergovernmental Panel on Climate Change (IPCC) AR-4 constructions (30) do not reproduce major elements of interdecadal variability. Furthermore, SST data in the equatorial central and eastern Pacific before the 1920s were sparse, and it is difficult to determine what form of Pacific warming took place during earlier phases of the Pacific Decadal Oscillation.

We do know that since 1960, especially since 1990, CPW events have become more prevalent and that there is a greater and earlier predictability of a CPW event than an EPW event. In addition, there is preliminary evidence that the character of Pacific cooling events has also changed during the past few decades. Future work will determine whether these differences result in changes in the characteristics of North Atlantic cyclones.

References and Notes

1. W. M. Gray, *Mon. Weather Rev.* **112**, 1649 (1984).
2. W. M. Gray, C. W. Landsea, P. W. Mielke Jr., K. J. Berry, *Weather Forecast.* **8**, 73 (1993).
3. J. B. Elsner, T. H. Jagger, *J. Clim.* **19**, 2935 (2006).
4. F. Vitart *et al.*, *Geophys. Res. Lett.* **34**, L16815 (2007).
5. R. A. Pielke Jr., C. N. Landsea, *Bull. Am. Meteorol. Soc.* **80**, 2027 (1999).
6. W. M. Gray, *Mon. Weather Rev.* **112**, 1669 (1984).
7. M. A. Saunders, R. E. Chandler, C. J. Merchant, F. P. Robert, *Geophys. Res. Lett.* **27**, 1147 (2000).
8. B. H. Tang, J. D. Neelin, *Geophys. Res. Lett.* **31**, L24204 (2004).
9. N. K. Larkin, D. E. Harrison, *Geophys. Res. Lett.* **32**, L13705 (2005).
10. K. Ashok, S. Behera, A. S. Rao, H. Y. Weng, T. Yamagata, *J. Geophys. Res.* **112**, C11007 (2007).
11. H. Y. Weng, K. Ashok, S. Behera, A. S. Rao, T. Yamagata, *Clim. Dyn.* **29**, 113 (2007).
12. H. Y. Kao, J. Y. Yu, *J. Clim.* **22**, 615 (2009).
13. J. S. Kug, F. F. Jin, S. I. An, *J. Clim.* **22**, 1499 (2009).
14. T. M. Smith, R. W. Reynolds, *J. Clim.* **17**, 2466 (2004).
15. E. M. Rasmusson, T. H. Carpenter, *Mon. Weather Rev.* **110**, 354 (1982).
16. C. W. Landsea *et al.*, in *Hurricanes and Typhoons: Past, Present and Future* (Columbia Univ. Press, New York, 2004), p. 177.
17. P. J. Webster, G. J. Holland, J. A. Curry, H. R. Chang, *Science* **309**, 1844 (2005).
18. K. Emanuel, *Nature* **436**, 686 (2005).
19. G. J. Holland, P. J. Webster, *Philos. Trans. R. Soc. London Ser. A* **365**, 2695 (2007).
20. S. B. Goldenberg, C. W. Landsea, A. M. Mestas-Nunez, W. M. Gray, *Science* **293**, 474 (2001).
21. J. B. Elsner, B. H. Bossak, X. F. Niu, *Geophys. Res. Lett.* **28**, 4123 (2001).
22. C. H. Ho, J. H. Kim, H. S. Kim, C. H. Sui, D. Y. Gong, *J. Geophys. Res.* **110**, D19104 (2005).
23. B. Efron, R. Tibshirani, *Science* **253**, 390 (1991).
24. www.cpc.noaa.gov/products/outlooks/hurricane2004/August/hurricane04.html

25. P. J. Webster, S. Yang, *Q. J. R. Meteorol. Soc.* **118**, 877 (1992).
26. P. J. Webster, *Meteorol. Atmos. Phys.* **56**, 33 (1995).
27. C. Torrence, P. J. Webster, *Q. J. R. Meteorol. Soc.* **124**, 1985 (1998).
28. www.ecmwf.int/services/dissemination/3.1/ Seasonal_Forecasting_ System_3.html
29. E. Di Lorenzo *et al.*, *Geophys. Res. Lett.* **35**, L08607 (2008).
30. G. A. Meehl *et al.*, *Bull. Am. Meteorol. Soc.* **88**, 1383 (2007).

Successful Conservation of a Threatened *Maculinea* Butterfly

J. A. Thomas,[1,2]* D. J. Simcox,[2] R. T. Clarke[2,3]

Globally threatened butterflies have prompted research-based approaches to insect conservation. Here, we describe the reversal of the decline of *Maculinea arion* (Large Blue), a charismatic specialist whose larvae parasitize *Myrmica* ant societies. *M. arion* larvae were more specialized than had previously been recognized, being adapted to a single host-ant species that inhabits a narrow niche in grassland. Inconspicuous changes in grazing and vegetation structure caused host ants to be replaced by similar but unsuitable congeners, explaining the extinction of European *Maculinea* populations. Once this problem was identified, UK ecosystems were perturbed appropriately, validating models predicting the recovery and subsequent dynamics of the butterfly and ants at 78 sites. The successful identification and reversal of the problem provide a paradigm for other insect conservation projects.

The conservation of insects poses formidable challenges (*1*). National extinction rates of temperate butterflies and other arthropods have recently exceeded those of terrestrial vertebrates and vascular plants (*2–6*), and population extinctions have frequently occurred on nature reserves where species' resources remained abundant (*6–8*). Moreover, every early attempt to conserve a declining butterfly failed because of inadequate understanding of the causes of decline (*7, 8*). In 1974, the International Union for Conservation of Nature therefore selected three butterflies, including the ~six species of *Maculinea* (Large Blues), as global flagships for lepidopteran conservation (*9*), advocating research into their ecology and the maintenance of source habitats (*10*); the longest-running initiative involves *Maculinea arion*.
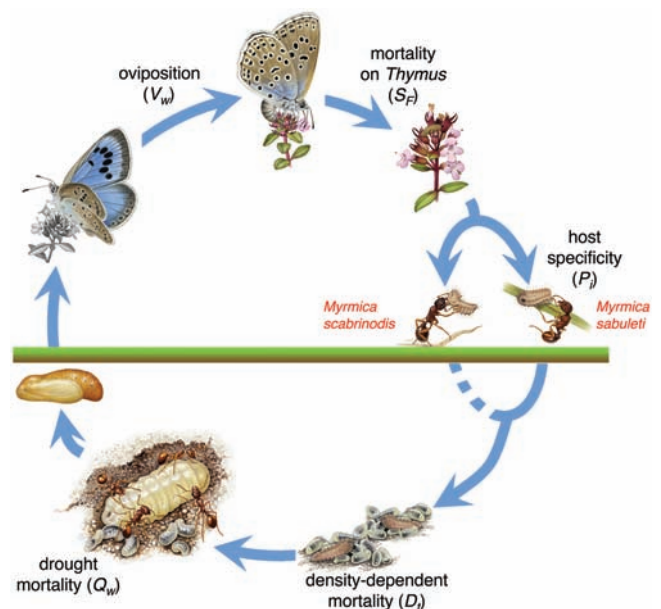
M. arion is an extreme specialist that switches from feeding on a plant to living as a social parasite inside *Myrmica* ant colonies during a 10-month larval instar and 3-week pupal period (Fig. 1). In the UK, *M. arion*'s population was estimated to include 91 colonies over the period of 1795 to the 1840s, declining to ~25 populations supporting tens of thousands of adults in 1950, and to 2 colonies of ~325 total individuals in 1972 before national extinction in 1979 (Fig. 2A) (*11, 12*). Nine sites were declared conserva-

tion areas from 1930 to 1969, which preserved *M. arion*'s *Thymus*- and *Myrmica*-rich grasslands but failed to slow extinctions (*12*).

To understand *M. arion*'s decline on superficially unchanged sites, annual variation in every factor causing mortality or reduced natality in the life cycle was identified and measured from 1972 to 1978 in its last UK population on Site X, Dartmoor (fig. S1) (*13*). We quantified 18 life-table parameters during 6 years of typical and extreme weather (table S1), including adult dispersal (*14*), oviposition choice and egg distribu-

tion (*15*), adult natality, egg and larval mortality on *Thymus* species, cannibalism on *Thymus* (*16*), adoption by *Myrmica* ant species (*17*), host specificity (*18*), queen effect on workers (*19*), and the carrying capacity of ant colonies (*20*). Mortality on *Thymus* (egg-larval instar$_{III}$) was low and had no influence on population dynamics (fig. S2), although the distribution of *Thymus* determined which *Myrmica* ant nests were accessible to larvae (*17*). Post-adoption larval instar$_{IV}$ mortality inside *Myrmica* nests was the key factor determining overall population changes (fig. S2), an analysis supported by phenomenological and spatial automata models (*16, 21*). We identified four causes of *M. arion* mortality at this stage: (i) availability of the preferred ant host species (*18*), (ii) presence/absence of queen ants (*19*), (iii) larval density within ant nests (*20*), and (iv) drought effects on host food availability (*22*). Factors (i) and (iii) were most variable: Five *Myrmica* species foraged beneath *Thymus* on Dartmoor and adopted instar$_{IV}$ larvae with probabilities proportional to worker abundance (*17*), but survival was 5.3 times higher in colonies of *Myrmica sabuleti* than with those of its congeners (*18*); population-scale survival with *M. sabuleti* decreased with larval density per nest (fig. S3).

Failure by female butterflies to lay their full potential of eggs amplified the population de-

[1]Department of Zoology, University of Oxford, South Parks Road, Oxford, OX1 3PS, UK. [2]Centre for Ecology and Hydrology, Maclean Building, Benson Lane, Crowmarsh Gifford, Wallingford, Oxfordshire, OX10 8BB, UK. [3]Centre for Conservation Ecology and Environmental Change, School of Conservation Sciences, Bournemouth University, Fern Barrow, Talbot Campus, Poole, Dorset BH12 5BB, UK.

*To whom correspondence should be addressed. E-mail: jeremy.thomas@zoo.ox.ac.uk

Fig. 1. Life cycle of *M. arion.* Adult butterflies oviposit on *Thymus* species flowers from June through July (model parameter V_w). Larval instars$_{I-III}$ feed on flowerheads for 3 weeks, with (including eggs) survival (S_F) depending on parasites, predation, and cannibalism. The small final instar$_{IV}$ larva abandons *Thymus* and is adopted into the underground nest of the first *Myrmica* ant worker to encounter it, with survival (P_t) depending on its adoption into primary (*M. sabuleti*) or secondary (*M. scabrinodis*) host-species' nests. *M. arion* larvae acquire ~98% of their final biomass eating ant brood and frequently experience density-dependent mortalities ($1 - D_t$) in nests that adopt more than 1 larva; mortalities in ant nests are amplified in drought years (Q_W). After 10 months, the larva pupates in the *Myrmica* nest, emerging as an adult 2 to 3 weeks later. [Illustrations by Richard Lewington]